Hydrobiologia (2011) 677:107–127
DOI 10.1007/s10750-011-0746-9

ANCHIALINE ECOSYSTEMS

The key role of the chemolimnion in meromictic cenotes of the Yucatan Peninsula, Mexico

Olmo Torres-Talamante · Javier Alcocer · Patricia A. Beddows · Elva G. Escobar-Briones · Alfonso Lugo

Received: 6 May 2010 / Accepted: 5 May 2011 / Published online: 19 May 2011

Abstract This study tests the ecological and physico-chemical effect of sharp density boundaries of meromictic lakes. The investigation was carried out in Nohoch Hol, an anchialine meromictic cenote situated 2.0 km inland from the Caribbean coast of the Yucatan Peninsula, Mexico. In situ physico-chemical parameters were recorded with a water quality datalogger at depth intervals of 0.5 m. In addition, seven water samples for determination of nutrients, bacterioplankton and phytoplankton in the water column were obtained using SCUBA. Bacterioplankton and phytoplankton densities are low, with concentrations consistent with the oligo- to ultraoligotrophic status of Nohoch Hol indicated by the low nutrient concentrations. The phytoplankton was dominated by the chlorophyte *Scenedesmus*. Maximum concentrations of bacterio- and phytoplankton were found at 10.0 m depth, the top of the chemolimnion. The similarity analysis clustered the samples in three defined groups: (a) the mixolimnion, (b) the mid- and bottom of the chemolimnion and the monimolimnion, and (c) the top of the chemolimnion. The principal component analysis explained over 85% of the total variance in two components (PC). PC1 was related to turbidity and the aggregation of the chlorophytes at the top of the chemolimnion. PC2 was related to dissolved oxygen and the accumulation of filamentous and total bacteria also at the top of the chemolimnion. The top of the chemolimnion acts as a boundary within the water column to the exchange of dissolved and particulate matter between the mixo and the monimolimnion and as an ecological zone with a crucial role in the biogeochemistry of Nohoch Hol.

Keywords Anchialine · Tropical lake · Karst · Sinkhole · Anoxia · Bacterioplankton · Phytoplankton · Nutrients

Guest editors: C. Wicks & W. F. Humphreys / Anchialine Ecosystems: reflections and prospects

O. Torres-Talamante
Colectividad RAZONATURA A.C., Luis G. de León No. 68. Copilco el Alto, Coyoacán, 04360 Mexico, DF, Mexico

J. Alcocer (✉) · A. Lugo
Proyecto de Investigación en Limnología Tropical, FES Iztacala, Universidad Nacional Autónoma de México, Av. de los Barrios No. 1, Los Reyes Iztacala, 54090 Tlalnepantla, Estado de México, Mexico
e-mail: jalcocer@servidor.unam.mx

P. A. Beddows
Department of Earth & Planetary Sciences, Northwestern University, 1850 Campus Drive, Evanston, IL 60208-2150, USA

E. G. Escobar-Briones
Instituto de Ciencias del Mar y Limnología, Universidad Nacional Autónoma de México, A.P. 70-305, Ciudad Universitaria, Coyoacán, 04510 Mexico, DF, Mexico

Introduction

The Yucatan Peninsula is the emergent portion of the carbonate Yucatan Platform, with Mesozoic and Cenozoic rocks in the interior, surrounded by concentric sequences of younger formations out to a ~10 km wide coastal Quaternary perimeter (Butterlin & Bonet, 1963; Lopez-Ramos, 1975; Weidie, 1985; Pindell, 1994). The Yucatan Peninsula is a karst physiographic/geologic unit extending southward to Belize and the Guatemala's Peten (Wilson, 1980) characterized by abundant caves and sinkholes particularly in the northern low-lands. Karst sinkholes are formed by dissolution and collapse of limestone. In the karst platform of the Yucatan Peninsula (SE Mexico) they are called cenotes.

Collapse and dissolution cenotes provide access to the density stratified coastal aquifer system, which includes a fresh water lens formed by infiltrating meteoric waters, floating on top of a saline water zone comprising intruding marine waters. The electrical conductivity (EC) of the "fresh" water lens along the Caribbean coast decreases exponentially with distance inland, with EC of 3.3 mS cm^{-1} in lotic conduit sites 4–10 km inland, and for sites less than 1 km inland the EC averages 18.2 ± 6.6 mS cm^{-1} (Beddows et al., 2007). Separating the fresh and saline waters is a defined mixing zone characterized by a halocline. Cenotes match the concept of dissolution lakes (Hutchinson, 1957), coastal lakes (Cole, 1979), as well as anchialine systems (Stock et al., 1986).

Cenote morphologies are varied. Some cenotes are cave entrances leading to groundwater, while others with open water pools are clearly sections of collapsed cave ceiling providing direct access to the extensive sub-horizontal turbulent flow conduits (Smart et al., 2006) of which more than 900 km have now been documented along the Caribbean coastal margin (QRSS, 2010). However, many cenotes are apparently not associated with conduits, and this is true particularly in the north-west of the Peninsula where the common cenote morphology is nearly circular 'pit' shaped open water bodies, with bell shaped bathymetries some of which extend down to 150 m depth (Beddows, 2003). There is a notable concentration of these large 50+ m diameter open water 'pit' cenotes overlying the K–T boundary aged Chicxulub impact crater that is buried beneath 500–1500 m of post-impact aged carbonates (Hildebrand et al., 1995; Connors et al., 1996; Pope et al., 1996). The study of several deep cenotes in the Yucatan Peninsula have provided new insight to limestone dissolution processes and sulfur redox phenomena due to their combined features of an open water column penetrating to the underlying modified marine intrusion, input of terrestrial organic debris, and restricted circulation of the bottom waters (Stoessell et al., 1989; Perry et al., 1995, 2009; Socki et al., 2002).

Hydrogeochemical studies of Yucatan cenotes have revealed some general differences between conduit flow sites, and lentic pit cenotes, although the differences are not categorical and exceptions are known. For sites 4+ km inland, the EC in lentic pit cenotes is lower by 1–2 mS cm^{-1} compared to nearby lotic cenotes. The interpretation of this offset was that turbulent flow entrained the water from the top of the mixing zone (here mixolimnion) and mixed it through the fresh water lens (Beddows, 2004; Beddows et al., 2007). Mixolimnia are also thicker in lentic pit cenotes. A sampling of 7 pit cenotes from the Caribbean coast of the Yucatan peninsula area showed that six of them had thick mixing zones which were 1–3+ m thick, while in contrast the lotic sites featured thin mixolimnia of 1 m or less (Beddows, 2004; Beddows et al., 2007). Socki et al. (2002) reported mixolimnia of 10 to >40 m in pit cenotes in the outer margin of the 'Ring of Cenotes' situated 50–55 km south from Gulf of Mexico coast.

The Yucatan coastal karst sinkholes (i.e., cenotes) can be classified in a variety of schema.

Meromictic

The cenotes are equally meromictic ponds or small lakes, wherever the collapse is deep enough for the water column to fully penetrate the meteoric lens and provide access to the underlying saline water.

Within standard limnological terminology, a meromictic water body includes higher electrical conductivity bottom water that is anaerobic, or at least with very low dissolved oxygen content (Lampert & Sommer, 1997; Wetzel, 2001). The stable density profile limits vertical mixing to the uppermost water layer, creating the limnological condition known as meromixis (Wetzel, 2001). In open water cenote pools, such as for Nohoch Hol considered here, we

find a permanent saline stratification, with an upper water layer of lower salinity and a perennial dense stratum of bottom saline water. The bottom saline layer in deeper cenotes corresponds to the monimolimnion and the upper water layer corresponds to the mixolimnion (Lewis, 1983, 1996; Wetzel, 2001). The halocline is the zone of sharp increase in salinity with depth, but given the concurrent sharp changes in oxygen, pH, and other chemical parameters, this halocline is more broadly a chemocline or chemolimnion upon the depth extension (Lampert & Sommer, 1997). As the saline water comes from an external source the meromixis is considered ectogenic (Wetzel, 2001).

Anchialine

These are anchialine systems sensus Stock et al. (1986) since marine water intrudes landward beneath a floating lens of meteoric groundwater. All hydrogeological aspects of the cenotes and caves within 8–10 km of the Caribbean coast are tidally influenced: instrumental monitoring and dye tracing have shown that the fresh and saline water velocities are tidally modulated, with periods of decoupled saline water recharge into the aquifer documented even while fresh water discharge continues (Beddows et al., 2002, Beddows, 2004). Cenote water table fluctuations are also tidal throughout the region with an overall exponential decrease with distance inland. For example, water table fluctuations at sites 5 km inland express $\sim$40% of the coastal micro-tidal $\sim$30 cm semi-diurnal amplitude (Beddows, 1999).

Lentic–lotic

Amongst the open water pool cenotes, Schmitter-Soto et al. (2002) classified those with horizontal turbulent flow as being lotic cenotes, within a limnological framework, whilst cenotes with circulation dominated by diffuse groundwater circulation principally via the limestone matrix, and fractures and fissures as lentic. Most of the cenotes found throughout the peninsula typically present characteristics intermediate between the lentic–lotic end-members proposed by Schmitter-Soto et al. (2002). The well studied cenotes of Angelita, and the three cenotes located in the Calica Quarry are all lentic pit cenotes in this scheme (Moore et al., 1992, 1993; Stoessell et al., 1993, 2002; Soteres, 2000).

The number of studies focused on anchialine meromictic cenotes of the Yucatan Peninsula remains small compared to the apparent number of sites. At least 950 cenotes are documented within the central portion of the Caribbean coast of the Peninsula in the state of Quintana Roo (QRSS, 2010), and the adjacent state of Yucatan boast an inventory of no less than 2241 (SEDUMA, 2010). In all cases, cenotes are the only natural access to fresh water supplies over the whole northern Peninsula, since the high permeability and infiltration through the young carbonates prevents the formation of any surface rivers. A range of hydrogeochemical aspects of the aquifer and cenotes are reported in Beddows (2004), Beddows et al. (2007), Moore et al. (1992, 1993), while Wilson & Morris (1994), Socki et al. (2002) and Stoessell et al. (2002) describe specifically pit shaped meromictic sites.

This study tests the ecological and physico-chemical effect of sharp density boundaries of meromictic lakes. Nohoch Hol was selected as the study anchialine meromictic cenote due to ease of surface access, and apparent lack of unique or outstanding features. Anchialine systems are amongst the lesser studied ecosystems globally, despite their high level of endemicity (e.g., Remipedia); provision of ecosystem services; ideal models of evolutionary and ecological processes; and in many cases the significant cultural and esthetic heritage associated with sites and landscapes where they occur (Iliffe, 2000; Glover & Earle, 2004; Boulton et al., 2008). As with all subterranean ecosystems and habitats, they are fragile and increasingly threatened by direct and indirect human impacts (Doehring & Butler, 1974; Boulton et al., 2008). This is particularly true along the Caribbean coast of the Yucatan Peninsula where a nearly continuous 100 km long urban zone is being planned for the next 30 years, supported by the tourism economy. The occurrence of persistent organic pollutants has recently been documented in the aquifer system along the Caribbean coast, with implications for the human and environmental health including that of the Meso American Barrier Reef System (MBRS), the second longest in the world (Metcalfe et al., 2011). This limnological study of the karst anchialine cenote, Nohoch Hol, will help establish representative limnological values for

cenotes on the eastern side of the Yucatan peninsula, while comparisons with similar coastal karst tropical/neo-tropical meromictic systems are also included to set the findings in a broader context.

Materials and methods

Cenote Nohoch Hol (aka Cenote Stram) is situated at 20.2809°N, 87.4026°W, 9 km north-east of the town of Tulum, and 2.0 km north-west inland from the Caribbean coast of the Yucatan Peninsula (Fig. 1). It lies in the southern portion of the "Holbox Fracture Zone—Xel-Ha Zone" hydrogeochemical/physiographic region where bicarbonate is the dominant ion associated with calcium in groundwater, and to the south towards the Sian Ka'an Biosphere Reserve is the transition zone beyond which gypsum dissolution adds calcium and sulfate ions to groundwater, affecting carbonate chemistry as it relates to limestone solubility (Perry et al., 2002, 2009). Nohoch Hol is formed in Quaternary limestone (Butterlin & Bonet, 1963; Lopez-Ramos, 1975; Weidie, 1985). This region has a tropical sub-humid moisture regime with a summer rainy season; the mean annual air temperature is 26°C ranging from 23 to 28°C (García, 1973). Along the Caribbean coast, the mean annual precipitation is >1500 mm (Instituto de Geografia, 1973). Evapotranspiration is poorly quantified, and estimates of aquifer recharge range through 30–70% of the mean annual precipitation (Beddows, 2004). The cenote is surrounded by tropical semi-deciduous forest <10 m tall (Rzendowski, 1981; Flores & Espejel, 1994).

The water surface in cenote Nohoch Hol is ~1 m below ground level, with a surface diameter of ~33 m and an area of 855 m^2, while at 8.5 m water depth the diameter increases to ~60 m (Fig. 1c). The basin has a maximum water depth of 17.8 m in the central portion. At 4.5 m depth on the south-east wall a horizontal dissolution conduit extends toward the coast for 186 m with the initial diver exploration

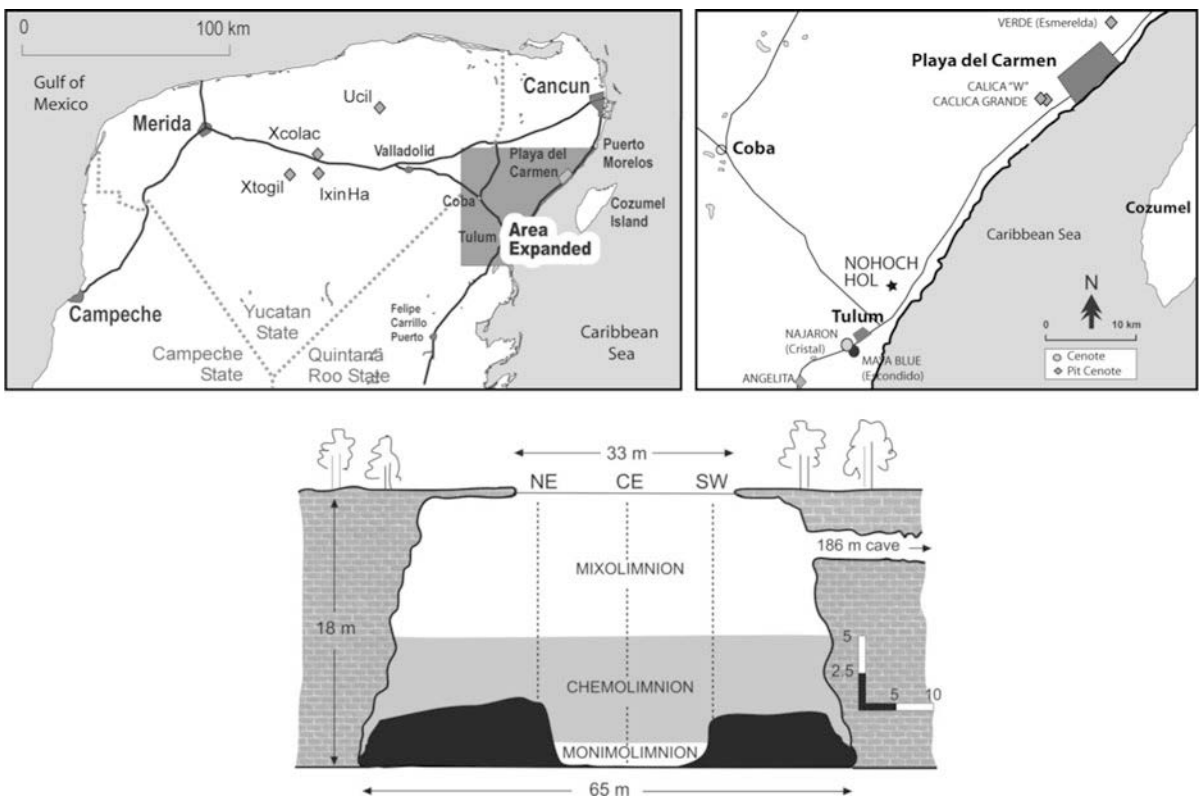

Fig. 1 Cenote Nohoch Hol and other cited cenotes of the Yucatan Peninsula. **a** Location of the Yucatan Peninsula, **b** location of cenote Nohoch Hol in the Caribbean coastal zone, **c** Cross-section of the Nohoch Hol anchialine pool

ending in air pockets, and no inland north-west passage has yet been documented (Bil Phillips personal communication). While there is potential for shallow horizonal flow through the cenote via conduit(s), the connectivity of the deeper basin generally appears to be poor, and groundwater exchange may be principally via pores, fractures, and fissures. The deeper basin of Nohoch Hol would therefore be equivalent to a groundwater flow-through lake. In the broader context, Nohoch Hol is flanked within 0.5 km to the north, east and south by flooded passages connected to the 67 km long Nohoch Nah Chich cave system (which was subsumed by connection into the now 180 km long Sac Aktun cave system), while there are short segments 100's of m long of other caves on the inland north-west side (QRSS, 2010). The tidal influence on the water table in Nohoch Hol was not monitored in this study, the nearby cenote Balam Can Chee situated 0.7 km to the north-east expresses 77% of the coastal tidal amplitude (Beddows, 1999).

Field data were collected in November between 11:00 and 12:00 h. In situ vertical profiles of physico-chemical parameters were recorded at depth intervals of 0.5 m using a calibrated Hydrolab DS3/SVR3 multi-parameter water quality datalogger. Manufacturer stated accuracy in depth to ±0.05 m, temperature to ±0.15°C, pH to ±0.2 units, electrical conductivity to ±1 mS cm^{-1}, dissolved oxygen (DO) to ±0.2 mg l^{-1}, redox potential (oxidation/reduction potential, ORP) to ±20 mV, and turbidity (no accuracy specified by manufacturer). Three vertical profiles were sampled along the long axis: northeast (NE), center (CE), and southwest (SW) with maximum depths of 12.5, 17.8, and 14.0 m, respectively.

Field assessment of the data showed horizontal homogeneity between the temperature, electrical conductivity, and dissolved oxygen profiles, and therefore the seven water samples for determination of nutrients, phytoplankton, and bacterioplankton in the water column were obtained in the center deepest station. The sampling focus was on the chemolimnion with water samples obtained at 10.0, 11.0, 12.0, and 13.0 m depth, while two were obtained from the mixolimnion at 2.0 and 8.0 m, and one from the monimolimnion at 16.0 m. Depth control for the water sampling was provided by a 0.5 m marked anchor line, suspended from a buoy in the center of the cenote. The open circuit SCUBA divers examined the sampling bottles at depth to ensure no ingress of water, prior to opening them. The sample bottles were held horizontal upon opening, allowing water to completely fill the bottle, which were then sealed at the sampling depth. Water samples included 500 ml in sterile Nalgene bottles for nutrients and phytoplankton, and 75 ml of water in dark-brown glass bottles for bacterioplankton. Samples for nutrient analysis were preserved on ice with analysis undertaken within 24 h following the protocols of Strickland & Parsons (1972), Parsons et al. (1984), and Stirling (1985). Nutrients included nitrogen ($N\text{-}NH_4$, $N\text{-}NO_2$, and $N\text{-}NO_3$), phosphorous (soluble reactive phosphorous –SRP– and total phosphorous –TP) and soluble reactive silica (SRSi). Phytoplankton samples were preserved with acid Lugol's solution to a final concentration of 1%. Bacterioplankton samples were 0.2 μm filtered, and neutralized with formalin to a final concentration of 2%.

Phytoplankton counts were made using settling chambers with a Leica inverted microscope at 40× and 100× magnification following the Utermöhl (1958) method. Larger 100 ml settling chambers were used with samples thought to have high phytoplankton density, and 10 ml chambers for the rest. Based on the assumption of random distribution in the chambers, 400 organisms were counted to achieve confidence limits of ±10% confidence limits, and counts were terminated with at least 100 individuals in each of the important species (Wetzel & Likens, 1979).

Samples for bacterioplankton were stained with DAPI (4′,6′-diamino-2-phenylindole), and 30 ml filtered onto black pre-stained 0.22 μm pore size Millipore membrane filters (Porter & Feig, 1980). Bacteria were counted using a Zeiss epifluorescence microscope under 1,250× magnification. Following the same criteria as for phytoplankton, 1000 bacteria were counted to obtain an accuracy of ±6% (Wetzel & Likens, 1979).

Kruskal–Wallis one-way analysis of variance on ranks and all pair-wise multiple comparison procedures (Dunn's method) were performed using Statistica v.6 (2001) and SigmaStat v.2.03 (1997) to test for differences between variables of the three profiles (NE, CE, and SW).

Density was computed using pressure, temperature, and salinity data according to the UNESCO International Equation of State (IES 80) as described

in Fofonoff (1985) with online software http://fermi.jhuapl.edu/denscalc.html.

Multivariate analysis was undertaken on the environmental and biological data from the seven sampling depths in the central station for which water samples were analyzed, in order to allow intercomparison of results down the water column. The Statistica release version 7 software package was used for the hierarchical clustering and PCA analysis. For these analyses the data were transformed as described in Table 1 to stabilize the variances of the various descriptors and to make them inter-comparable despite their difference in units.

The similarity of depths was computed using the single linkage agglomerative clustering method. Euclidean distance was the measure of association between pairs of objects. Visual examination of the resulting dendrogram was used to subjectively define the resulting clusters.

Primary component analysis (PCA) was used to reduce the dimensionality of data and to transform interdependent variables into significant and independent components. This method has been extensively described in Gauch (1982), Legendre & Legendre (1998), and Borcard et al. (2011) and was applied here to the transformed and normalized data (Table 1).

Fig. 2 Physico chemical profiles in Nohoch Hol of **A** electrical conductivity, **B** temperature, **C** dissolved oxygen, **D** redox potential, **E** pH, **F** turbidity, and **G** density. Symbols are: *square* northeast profile, *circle* central, and *triangle* southwest. *Crossbars* indicate manufacturer sensor accuracy. Accuracy for turbidity and calculated density not available. Chemolimnion shown by the *gray area*

Results

Physicochemistry

The electrical conductivity profiles show three distinct water layers in Nohoch Hol which we use here to delimit the strata (Fig. 2A).

Mixolimnion (0.0–9.0 m)

The mixolimnion was characterized as a "freshwater" layer with an average of 5.0 ± 0.8 mS cm^{-1} (total dissolved solids—TDS $= 2.8 \pm 0.4$ g l^{-1}; Fig. 2A). The most significant physico-chemical features of the mixolimnion are the continuous temperature increase (Fig. 2B) between the surface and the base of the layer (9 m depth) and the dissolved oxygen clinograde profile decreasing from 7.3 mg l^{-1} (90% DO saturation) at the surface to 1.0 mg l^{-1} (10% DO saturation) at the base of the

Table 1 List of the environmental factors and the biological components considered in the cluster analysis and the transformations applied to each

Environmental factor	Abbreviation	Transformation	Biological component	Abbreviation	Transformation
Depth	Z(m)	No transformation	Bacteria*	Bac	Fourth root
Temperature	Tem	Natural logarithm	Filamentous bacteria*	Fil	Fourth root
Dissolved oxygen*	DO	Natural logarithm + 1	Cocci*	Coc	Fourth root
Electrical conductivity*	K25	Natural logarithm	Total bacteria	BacTot	Fourth root
Oxidation reduction	ORP	Natural logarithm	Chlorophytes*	Chlor	Fourth root
Potential*		+120, squared root	Bacilarophytes*	Baci	Fourth root
pH	pH	No transformation	Cyanophytes*	Cyan	Fourth root
Turbidity*	Tur	Natural logarithm	Total phytoplankton	PhyTot	Fourth root
Ammonium*	NH_4	Natural logarithm + 1			
Nitrite	NO_2	Natural logarithm + 1			
Nitrate*	NO_3	Natural logarithm + 1			
Phosphate	PO_4	Natural logarithm + 1			
Total phosphorus	TP	Natural logarithm + 1			
Silicate dioxide	SiO_2	Natural logarithm			

Abbreviations cross-list to those in Figs. 5 and 6. The Principal components analysis considered only those factors and components marked with an asterisk

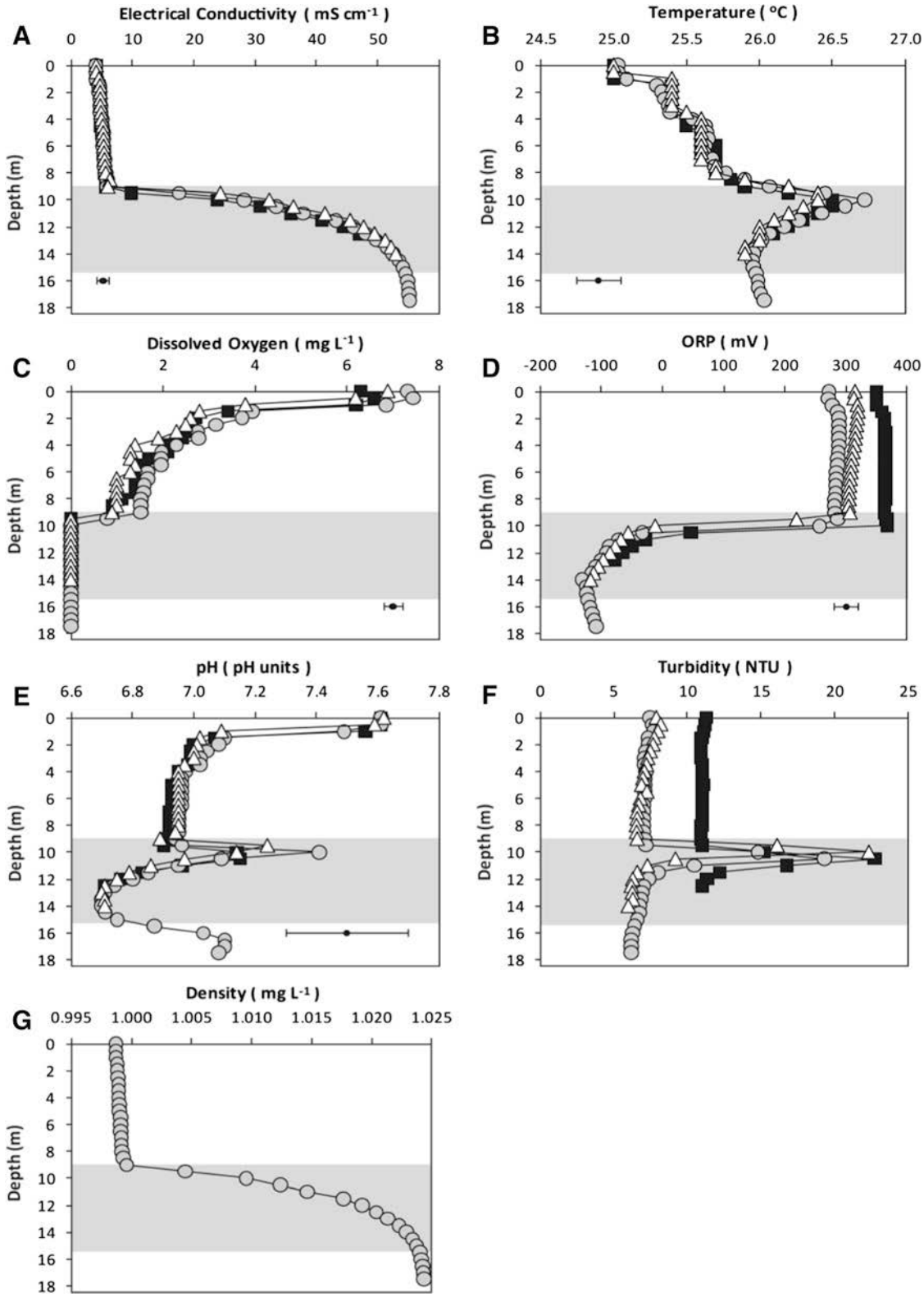
A
Electrical Conductivity (mS cm-1)
0 10 20 30 40 50
B
Temperature (°C)
24.5 25.0 25.5 26.0 26.5 27.0
C
Dissolved Oxygen (mg L-1)
0 2 4 6 8
D
ORP (mV)
-200 -100 0 100 200 300 400
E
pH (pH units)
6.6 6.8 7.0 7.2 7.4 7.6 7.8
F
Turbidity (NTU)
0 5 10 15 20 25
G
Density (mg L-1)
0.995 1.000 1.005 1.010 1.015 1.020 1.025
Depth (m)
0 2 4 6 8 10 12 14 16 18

mixolimnion (Fig. 2C). The ORP varied little through the mixolimnion with an overall average value of 318 ± 35 mV (Fig. 2D). The pH descended rapidly in the first 2 m from 7.5 to 7.0, but below this depth pH remained stable all the way down to the base of the mixolimnion (Fig. 2E). Turbidity was low (8.4 ± 1.8 NTU) (Fig. 2F) along the mixolimnion.

The three profiles across the open water pool were horizontally homogeneous, except for the ORP and turbidity that attained higher values (364 mV, 11 NTU) in the NE than in the central and the SW profiles (285 and 312 mV, respectively, 7 NTU for both). The NE, CE, and SW profiles were significantly different for ORP ($H = 49.939$, $P \leq 0.001$) as well as for turbidity ($H = 37.620$, $P \leq 0.001$).

Chemoliminion (9.0–15.5 m)

The chemolimnion was characterized by sharp gradients in all parameters (Fig. 2A–G). The upper boundary (9.0 m) of the chemolimnion is neatly defined as an electrical conductivity inflection point at 6.7 mS cm^{-1}, whereas the lower boundary (15.5 m) is less distinct but assessed here to occur once a nearly isohaline and nearly marine water was observed, corresponding to 54.6 ms cm^{-1}. Descending through the chemolimnion, temperature, and turbidity have marked maxima near the top of the chemolimnion, whereas DO and ORP decreased abruptly (Fig. 2B–D, F).

A temperature maximum of 26.7°C occurs at 10.0 m, which is 0.6°C higher than at 9.0 m at the base of the mixolimnion, and 0.7°C higher than the monimolimnion. The pH showed a polymodal profile shifting from neutrality to slightly basic (7.4) at the top of the chemolimnion and neutral to slightly acidic (6.7) at the base of chemolimnion (Fig. 2E). The ORP decreased from positive values >285 mV, to negative ones of −125 mV, while DO declined precipitously to anoxia. The three profiles were horizontally homogeneous at the chemolimnion, except ORP and turbidity. The three chemolimnion ORP profiles were significantly different ($H = 10.207$, $P = 0.006$), while turbidity displayed significant differences only between the NE and the other two profiles ($H = 9.310$, $P = 0.01$).

Monimolimnion (>15.5)

The monimolimnion was reached only in the central and deepest profile. It was saline with 55.1 ± 0.1 mS cm^{-1} (TDS = 36.6 ± 0.1 g l^{-1}) and therefore similar to seawater electrical conductivity (Fig. 2A). The temperature was 26°C. The DO concentration was below the limit of detection of the probe (<0.2 mg l^{-1}), the ORP negative (−107 mV) and the pH close to neutrality (Fig. 2C–E).

Nutrients

Nutrient concentrations in the mixolimnion were homogeneous. $N\text{-}NO_3$ was the nutrient with the highest concentration reaching 34.8 μM, while SRP was below the analytical detection limit of 0.02 μM (Fig. 3A, B, respectively). $N\text{-}NH_4$ and SRSi were low with 0.9–2.4 μM and 91.0–101.9 μM, respectively (Fig. 3A, C, respectively). $N\text{-}NO_3$ displayed the highest concentrations in the mixolimnion, diminishing within the chemolimnion, and the minimum at the monimolimnion. $N\text{-}NH_4$ reached the highest values in the chemolimnion diminishing towards the monimolimnion while the mixolimnion held the lowest concentrations (Fig. 3A; Table 2).

SRP, TP, and SRSi showed two peaks, a small one at 10.0 m and a larger at or 13.0 m (Fig. 3B, C; Table 2). Lastly, nutrients in the monimolimnion were generally low: $N\text{-}NO_3 = 0.116$ μM, SRP = 0.1 μM, TP = 0.4 μM, SRSi = 160.0 μM. The one exception was $N\text{-}NH_4$ that was relatively high at 9.3 μM (Fig. 3A, C; Table 2).

Bacterioplankton and phytoplankton

A total of three bacterial morphotypes were recognized in the water samples of cenote Nohoch Hol: bacillus, cocci, and filamentous bacteria. Of these morphotypes bacillus is dominant representing >80% throughout the water column (Fig. 4A). The bacterioplankton density increases with depth from 8.3×10^3 cells ml^{-1} at 2.0 m to 35.2×10^3 cell ml^{-1} at 10.0 m (Fig. 4A), which is the same depth of the phytoplankton maximum. Within the mixolimnion, the bacterioplankton density increases slightly towards the top of the chemolimnion (Table 3; Fig. 4A). Within the chemolimnion, the bacterioplankton displays two maxima at 10.0 m with 35.2×10^3 cells ml^{-1} and at 12.0 m with 23.1×10^3 cells ml^{-1}, matching the $N\text{-}NH_4$ peaks at the same depths. In the monimolimnion, the bacterioplankton density attains similar

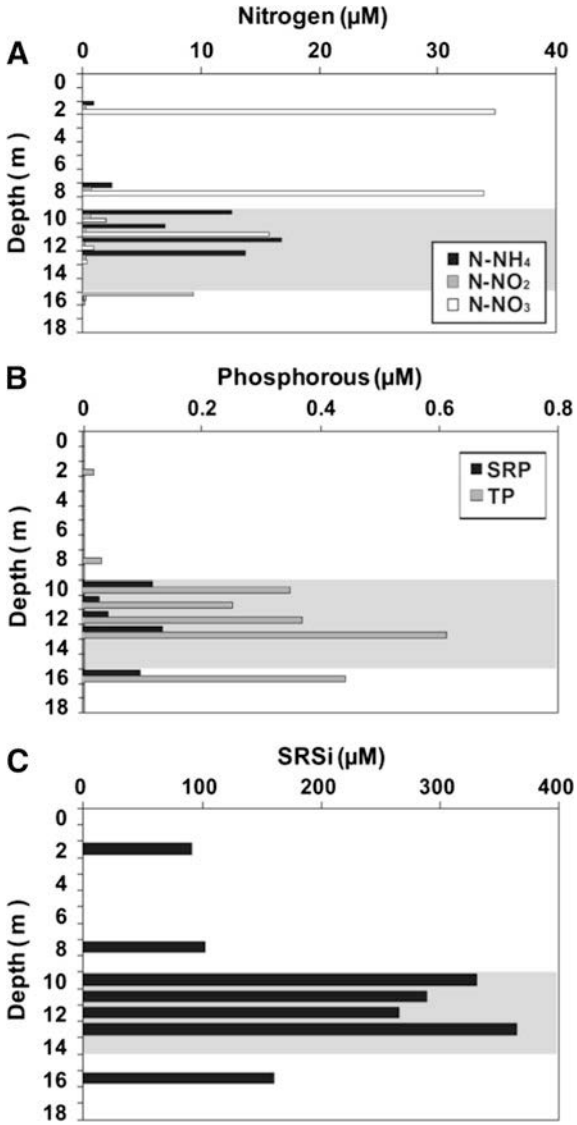

Fig. 3 Nutrient concentration profiles in Nohoch Hol of **A** nitrogen forms, **B** phosphorus forms, and **C** soluble reactive silica (SRSi). Chemolimnion shown by the *gray area*

values to those found in the mixolimnion with 12.9×10^3 cells ml^{-1}.

Nohoch Hol's phytoplankton includes 11 taxa belonging to three divisions: Chlorophyta (*Chlorella*, *Monoraphidium*, *Scenedesmus*), Bacillariophyta (*Cyclotella*, two species of *Navicula*, three species of *Nitzchia*), and Cyanophyta (*Chroococcus*, *Phormidium*). Chlorophyta is the dominant taxon with 96% of the total phytoplankton abundance (Table 4), followed by Bacillariophyta (3.8%) and Cyanophyta (0.2%). Among the Chlorophyta, a single genus, *Scenedesmus,* comprises more than 93% of the total phytoplankton abundance (21.9×10^3 cells ml^{-1}). As a consequence, the Shannon–Wiener diversity index is very low 0.27.

Scenedesmus and *Cyclotella* are dominant in the mixolimnion. The density of the phytoplankton (Fig. 4B) increases towards the top of the chemolimnion from 0.48×10^3 cells ml^{-1} at 2 m up to 20.7×10^3 cells ml^{-1} at 10.0 m where *Scenedesmus* composes >99% (20.5×10^3 cells ml^{-1}) of the total abundance. At 11.0 m the phytoplankton density reaches 0.058×10^3 cells ml^{-1} with *Cyclotella* as the dominant component with 90%. Below this depth, there is no phytoplankton.

Similarity and PCA

The dendrogram of the cluster analysis based on the environmental variables and the biological components for the seven depths in the central station in Nohoch Hol reveals three groups (Fig. 5). Group 1 corresponds to depths 2 and 8 m, both being mixolimnion depths. Group 2 includes depths 11, 12, 13, and 16 m, which begin in the mid-chemolimnion grading downwards into the monimolimnion. There is a step-wise increase in linkage distance with the 13 m (chemolimnion) and 16 m (monimolimnion) samples being closest, and then adjoining 12 m depth, and then finally 11 m depth. Group 3 includes only the 10 m depth, which corresponds to the upper boundary of the chemolimnion.

The principal component analysis (PCA) showed that the eigenvalues of the two first principal components represent up to 85.39% of the total variance (PC1 53.40%; PC2 31.99%) of the observations (Fig. 6). This percentage increases to 95.72% when a third component is included. The high-value with two components makes us confident that our interpretation of the first pair of axes extracts most relevant information from the data. Figure 6 shows that component 1 is based on the related and well-correlated variables of turbidity and the biological component Chlorophyta, which in turn are related to algae aggregated in the sharp gradients at the top of the chemolimnion in Nohoch Hol. The positive values on component 1 correspond to the decrease of turbidity and density of the Chlorophyta, and the

Table 2 Summary of physico-chemical and biological variables for Nohoch Hol

Variable	Units	Depth						
		Mixolimnion		Chemolimnion				Monimolimnion
		2 m	8 m	10 m	11 m	12 m	13 m	16 m
Temperature	°C	25.4 ± 0.0	25.7 ± 0.0	26.5 ± 0.2	26.3 ± 0.1	26.1 ± 0.1	26.0 ± 0.0	26
pH	pH units	7.0 ± 0.0	6.9 ± 0.0	7.2 ± 0.2	6.9 ± 0.1	6.8 ± 0.0	6.7 ± 0.0	7
Dissolved oxygen	mg l^{-1}	3.0 ± 0.6	1.2 ± 0.3	BDL	BDL	BDL	BDL	BDL
Electrical conductivity	mS cm^{-1}	4.7 ± 0.1	5.6 ± 0.1	28.1 ± 4.2	38.3 ± 2.8	46.0 ± 1.7	50.5 ± 1.1	54.9
ORP	mV	324	317	204	−56	−81	−107	−119
Turbidity	NTU	8.6 ± 2.0	8.2 ± 2.4	17.4 ± 4.2	11.5 ± 4.8	8.3 ± 2.6	6.6 ± 0.4	6.3
N-NO_3	µM	34.8	33.9	2.0	15.7	0.8	0.3	0.1
N-NO_2	µM	0.2	0.6	0.5	0.2	0.1	0.2	0.2
N-NH_4	µM	0.8	2.4	12.5	6.9	16.7	13.6	9.2
DIN	µM	35.8	36.9	15	22.8	17.6	14.1	9.5
SRP	µM	BDL	BDL	0.1	BDL	BDL	0.1	BDL
TP	µM	BDL	BDL	0.3	0.2	0.3	0.6	0.4
SRSi	µM	90.9	101.9	330.9	288.2	264.8	364.2	160.1
Phyto-plankton	$\times 10^3$ cell ml^{-1}	480	770	20,700	5	BDL	BDL	BDL
Bacterio-plankton	$\times 10^3$ cell ml^{-1}	8.3	11.8	35.2	12.1	23.1	10.1	12.9

ORP oxidation reduction potential, *N-NO_3* N as nitrates, *N-NO_2* N as nitrites, *N-NH_4* N as ammonia, *SRP* soluble reactive phosphorous, *TP* total phosphorous, *SRP* soluble reactive phosphorous, *Si–SiO_2* Si as soluble reactive silica, *BDL* below detection limit, *NTU* nephelometric turbidity units

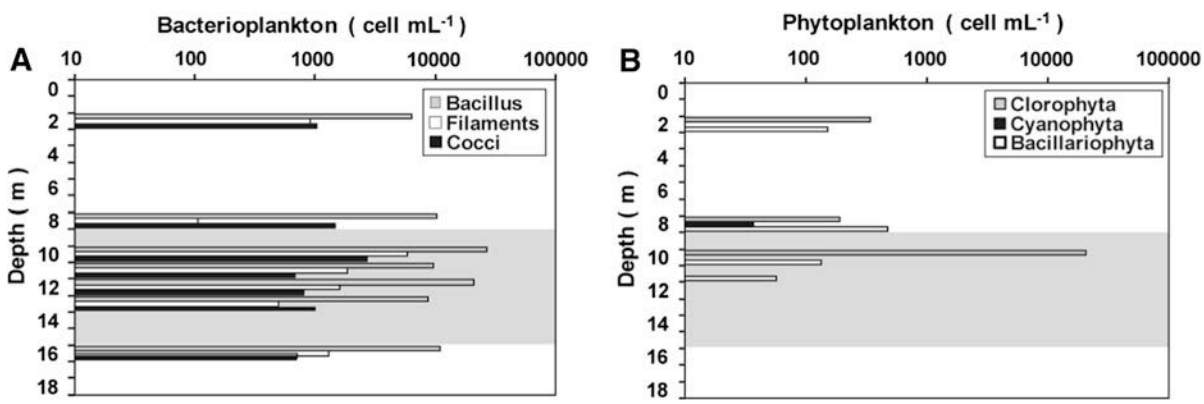

Fig. 4 Bacterioplankton and phytoplankton density at sampled depths in Nohoch Hol of **A** bacterioplankton morphotypes, **B** diatoms, cyanophyta, and chlorophyta. Chemolimnion shown by the *gray area*. *Horizontal axis* is plotted in log format

negative values the increase in values of these two variables. Component 2 is represented by the dissolved oxygen and the densities of filamentous bacteria and total bacteria. The positive values of this component characterize the layer with larger dissolved oxygen content and lower bacterial densities.

Discussion

Seasonality of physical conditions and biological and chemical processes is important in limnology. The interpretation in the present limnological study of Nohoch is provided as a snap-shot of the biogeochemistry of an eastern Yucatan Peninsula cenote.

Table 3 Bacterioplankton density and morphotype composition comparison of Nohoch Hol with other Yucatan Peninsula cenotes

Cenote	Classification	Lentic or lotic	Water layer	Density ($\times 10^3$ cell ml^{-1})	Bacillus (%)	Filamentous (%)	Cocci (%)	Source
Nohoch Hol	Meromictic	Lentic	Mixolimnion	8.3–11.7	81.4	7.0	11.6	1
	Anchialine		Chemolimnion	35.2–10.1	82.2	11.2	6.7	
			Monimolimnion	12.9	84.4	10.1	5.5	
Casa	Meromictic	Lotic	Epicline*	0.5	64.1	35.9	0	2, 3
	Anchialine		Halocline*	~0.75	ND	ND	ND	
			Hypocline*	~0.8	64.8	35.2	0	
Escondido	Holomictic	Lotic	Surface	3.2	27.7	66.8	5.5	2, 3
			Bottom		16.2	83.8	0	
Aktun Ha (Car Wash)	Holomictic Anchialine	Lotic	Water column	~0.9	19.4	80.6	0	2, 3
Cristal	Holomictic	Lotic	Water column	~2.1	83.5	5.9	10.6	2, 3
Nohoch Nah Chich	Holomictic	Lotic	Water column	~1.2	81.8	18.2	0	2, 3

Reference sources: 1 = this study, 2 = Alcocer et al. (1999), 3 = Sánchez et al. (2002); *BDL* below detection limit, *ND* no data available

Morphology and circulation

Nohoch Hol is a circular collapse into a deeper void space. The cenote floor happens to be within the present monimolimnion, and is now mantled by the rocky collapse debris combined with organic tropical forest liter. The speleogenesis can only be speculated, with potentially collapse into an underlying void associated with deep platform dissolution (Perry et al., 2009), or the collapse may overlie a ~20 m + depth tier of conduits identified in this region (Smart et al., 2006).

The nearly isohaline mixolimnion indicates that the upper waters are able to mix and thus have some form of circulation. This may relate simply to stratified horizontal flow associated with the shallow 4.5 m conduit(s) of this site. It must equally be considered that the mixolimnion may overturn, partial or complete, driven by seasonal and/or diurnal temperature cycles, and energy losses from evaporative cooling. The small, but concomitant step-wise increases in electrical conductivity and temperature and the decreases in DO suggest overprinting of partial overturning events, each penetrating to different depths. The relatively large surface diameter provides for an adequate fetch, combined with the water table within ~1 m of the ground surface, may be key characteristics allowing for overturning of the mixolimnion to occur in Nohoch Hol, and not in other cenotes of the region where the water surface is smaller and typically 2–10 m below ground level. Future study including repeat water column profiles over time, dye tracing, or instrumental measurement of flow, will clarify the nature of the mixolimnion circulation.

In contrast, the data for the chemolimnion and monimolimnion provide no evidence for circulation. The thermal maximum within the chemolimnion supports near-lentic conditions at 10+ m water depth. Nohoch Hol is therefore an interesting case with limnological vertical stratification, with this study indicating lentic conditions dominated by diffuse groundwater flow in the chemolimnion and monimolimnion, while some degree of circulation occurs in the surface mixolimnion waters.

Electrical conductivity

The electrical conductivity of the Nohoch Hol mixolimnion is 5.0 ± 0.8 mS cm^{-1} (TDS = 2.8 ± 0.4 g l^{-1}) which is consistent with the electrical conductivity in lotic conduit-connected cenotes at similar distance inland from the coast (Beddows et al., 2007). In lotic conduit sites, it was suggested (Beddows, 2004; Beddows et al., 2007) that the higher electrical conductivity was due to turbulent mixing of

Table 4 Comparison of phytoplankton taxonomic richness (*S*), density and composition of some Yucatan Peninsula cenotes

Cenote	Classification	Lentic or lotic	Taxonomic richness (*S*)	Diversity (H')	Density ($\times 10^3$ cell ml^{-1})	Phytal composition	%	Source
Nohoch Hol	Meromictic/ Anchialine	Lentic	11	0.27	21,900	Bacillariophyta	3.7	1
						Chlorophyta	96	
						Cyanophyta	<5	
Casa	Meromictic/ Anchialine	Lotic	50	ND	ND			2
Nohoch Nah Chich	Holomictic	Lotic	41	ND	ND			2
Escondido	Holomictic	Lotic	46	ND	ND			2
Cristal	Holomictic	Lotic	33	ND	ND			2
Aktun Ha	Holomictic	Lotic	32	ND	ND			2
Xlaka		Lentic	ND	ND	5,900–25,000	Bacillariophyta	<5	3
						Chlorophyta	<5	
						Cyanophyta	92.9	
						Euglenophyta	<5	
						Crypto	5.2	
						Chryso	<5	
Ixin-Ha		Lentic	ND	ND	16,000–7,900,000	Bacillariophyta	<5	3
						Chlorophyta	31.7	
						Cyanophyta	66.6	
						Cryptophyta	<5	
						Chrysophyta	<5	
						Pyrrophyta	<5	
Xtogil		Lentic	88	0.9	1.9	Bacillariophyta	79	4
						Chlorophyta	13.2	
						Cyanophyta	5.3	
						Euglenophyta	<5	
						Cryptophyta	<5	
						Rhodophyta	<5	

Reference sources: 1 = present study, 2 = Sánchez et al. (2002), 3 = Díaz-Arce et al. (2001), 4 = López-Adrián and Herrera-Silveira (1994); *ND* no data available

chemolimnion water upwards into the mixolimnion. This is in contrast to the electrical conductivity of other lentic pit cenotes of the Caribbean coast region, with values 1–2 mS cm^{-1} than in the lotic sites, although there was overlap in the electrical conductivity ranges and sampling of other sites has only included lentic pit cenotes situated at $\sim$4 km inland or more, whereas Nohoch Hol is at 2 km inland. In the case of Nohoch Hol the mechanism for slightly elevated electrical conductivity relative to their lentic cenotes similarly positions may be turbulent horizontal flow through the shallow conduits at this site. However, it is also considered that partial or complete overturning of the mixolimnion may also elevate the electrical conductivity, in distinction to other lentic pit cenotes of this region. Seasonal overturning of the mixolimnion, either partial or complete, has been shown to affect the depth and the thickness of mixolimnion and chemolimnion in other tropical lentic systems (Lewis, 1973; Salas & Martino, 1991; Talling & Lemoalle, 1998; Barbosa & Padisák, 2002; Tavera & Martínez-Almeida, 2005). In meromictic systems like Nohoch Hol, such a convective circulation mixes the top of the chemolimnion upwards, increasing the electrical conductivity of the mixolimnion, and also reducing the depth of the chemolimnion.

In coastal aquifers, the depth of the chemolimnion increases with distance inland as function of aquifer

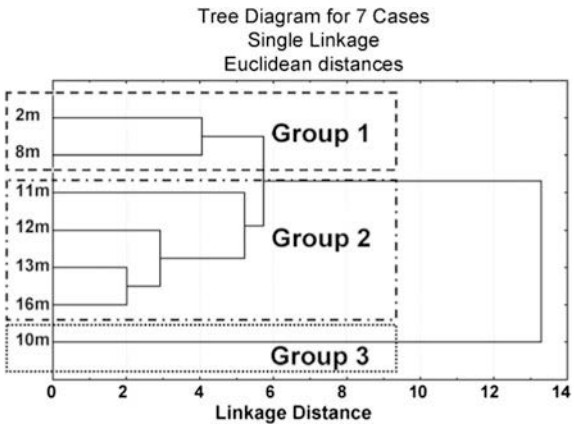

Fig. 5 Dendrogram showing the agglomerative clustering of the seven depths of Nohoch Hol in three groups: *1* mixolimnion, *2* mid-chemolimnion + monimolimnion, and *3* top of the chemolimnion

permeability provided by interconnected pores, fractures, and integrated dissolution conduit networks (Fetter, 1972, 1994). The chemolimnion in lotic conduit sites in the Caribbean coast region occurs at 10–10.5 m depth, and with a thickness of 0.5–3 m (Beddows, 2004: Figure 4.1). The top of the chemolimnion in Nohoch Hol begins somewhat shallow at 9.0 m, and is thick, measuring 6.5 m (Fig. 7A). The thickness of the chemolimnion in Nohoch Hol is greater than lotic conduit sites, but thinner than other known poorly connected lentic pit shaped cenotes such as Cenote Grande with a +13 m thick chemolimnion (Fig. 7A; Table 5). A consequence of reduced depth of the chemolimnion associated with overturning is a concurrent increased thickness as observed in other tropical lentic systems (Lewis, 1973; Salas & Martino, 1991; Talling & Lemoalle, 1998; Barbosa & Padisák, 2002; Tavera & Martínez-Almeida, 2005). Our observations of somewhat elevated electrical conductivity in the mixolimnion, combined with a shallow and thick chemolimnion, underline the need for temporal physico-chemical observations in Nohoch Hol to assess the occurrence of overturning in this site, which would be a first documentation of this fundamental limnological process in a cenote.

The monimolimnion presented an electrical conductivity of 55.1 ± 0.1 mS cm^{-1} (TDS $= 36.6 \pm 0.1$ g l^{-1}) which is similar to typical coastal marine waters along the Caribbean coast (Merino Ibarra & Otero Dávalos, 1991).

Temperature

The temperatures of the mixolimnion and the monimolimnion in Nohoch Hol reflect the temperatures of the source waters: meteoric/groundwater and marine,

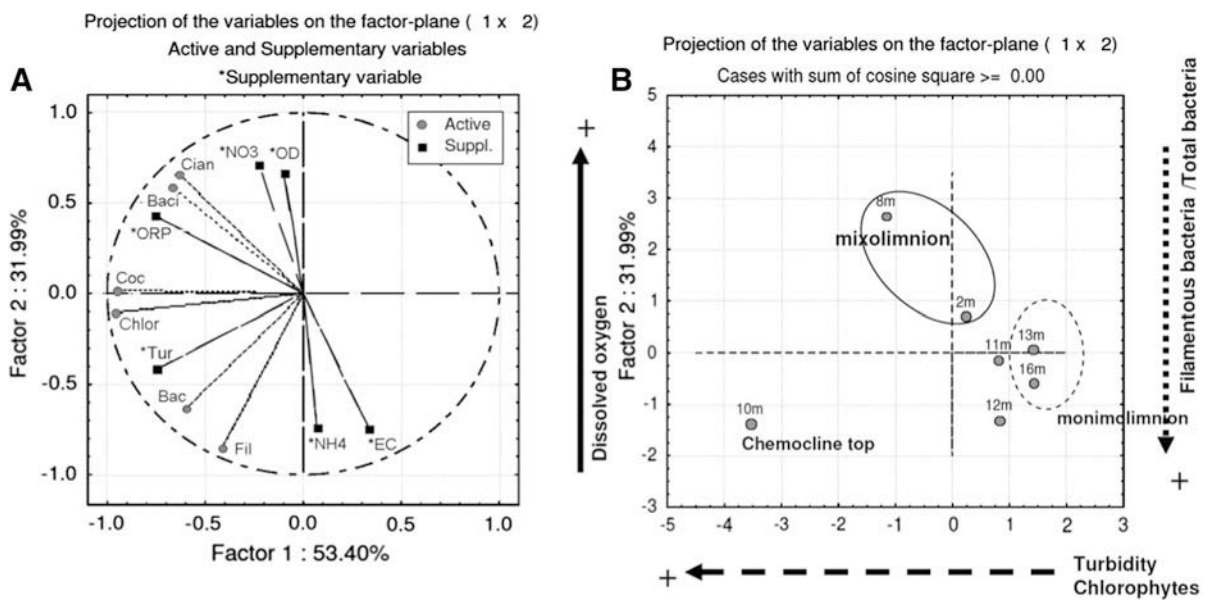

Fig. 6 **A** Loadings of the 10 PCA experimental variables. **B** Scores of the cases on the factor-plane (1 × 2) defined by principal components 1 and 2 obtained by the 10 experimental variables

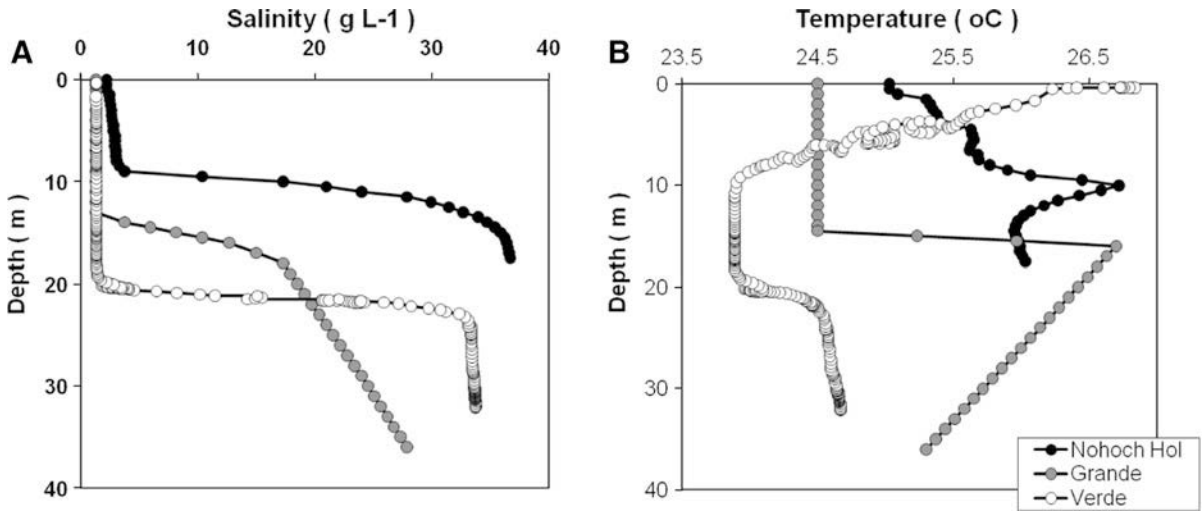

Fig. 7 Comparative **A** salinity and **B** temperature profiles from three different meromictic cenotes of the Yucatan Peninsula: Nohoch Hol, Grande (Skiles et al., 1997), and Verde (Beddows, 2004)

Table 5 Physical and chemical variables from some meromictic systems of the world

	Variable	Units	Yucatan, Mexico—Tropical			Florida, USA—Subtropical	Bahamas—Subtropical		NW Australia—Tropical
			NH	CG	CV	JS	CP	BH	BS
Mixolimnion	Salinity	g l^{-1}	2.77	1.3	0.8	25	2.9	12	19
	Temperature	°C	25	24.5	30	~30	30.7	29	22
	Dissolved oxygen	mg l^{-1}	7.3	ND	ND	~6	7.5	6	~8
	pH	pH units	7	ND	ND	~8	7.7	8.5	7.5
	ORP	mV	300	ND	ND	ND	ND	ND	175
Chemolimnion	Halocline depth	m	9	15.2	21	~10	8	17.8	7.5
	Salinity	g l^{-1}	25.5	17.2	17.5	~30	30	25	32
	Temperature	°C	26.7	26.7	28	~20	24.1	36	25
	Dissolved oxygen	mg l^{-1}	<1	ND	ND	5 to <1	0.42	<1	<1
	pH	pH units	6.7–7.4	ND	ND	~9.7	6.5	8.6–6.45	6.9
	ORP	mV	−118	ND	ND	ND	ND	ND	−125
Monimolimnion	Salinity	g l^{-1}	36.6	27.8	33.3	35	30.6	35	34
	Temperature	°C	26	25.3	25	17	22.3	26	26
	Dissolved oxygen	mg l^{-1}	<1	ND	ND	<1	0.18	<1	<1
	pH	pH units	7	ND	ND	~7.5	6.6	7.5	6.9
	ORP	mV	−111	ND	ND	ND	ND	ND	−125

Site locations are: *NH* Nonoch Hol, eastern Yucatan Peninsula (present study); *CG* Cenote Grande, eastern Yucatan Peninsula from Stoessell et al. (1993); *CV* Cenote Verde, eastern Yucatan Peninsula from Wilson & Morris (1994); *JS* Jewfish Sink, Gulf Coast of Florida from Garman & Garey (2005); *CP* Cottage Pond, North Caicos Island, Bahamas from Koenemann et al. (2004); *BH* Black Hole, South Andros Island Bahamas from Schwabe & Herbert (2004); *BS* Bundera Sinkhole, northwest Australia from Humphreys (1999) and Humphreys et al. (1999)

respectively. In the eastern Yucatan Peninsula, the average annual air temperature is 26°C and the coastal shallow Caribbean surface water is 27°C (Merino Ibarra & Otero Dávalos, 1991). Such groundwater–climate–marine thermal relationships are typical of anchialine coastal sites, with cold

intruding marine waters in locations such as the Bahamas where the ectogenic source is the cold near-shore currents flowing through the Tongue of the Ocean passage (Table 5; Schwabe & Herbert, 2004; Whitaker & Smart, 1997).

A thermal anomaly sensu Stoessell et al. (2002) is present in Nohoch Hol where a temperature maximum is contained within the chemolimnion (Fig. 2B). Similar features had been described from other open water meromictic cenotes in the Yucatan Peninsula (Stoessell et al., 2002; Beddows, 2004; Beddows et al., 2007) and the Bahamas (Schwabe & Herbert, 2004) (Table 5). Stoessell et al. (2002) consider that biological activity, heliothermic heating and/or geothermal convective cells may give rise to the subsurface excess temperature at and within the chemolimnion. These three processes are of very different scale and the occurrence of one does not exclude the others and could be complementary. In agreement with Beddows (2004) and Beddows et al. (2007), we consider heliothermic heating through turbidity (Fig. 2B, F) as the explanation for the thermal anomaly in Nohoch Hol. Heliothermic heating occurs where incoming light penetrates a transparent water column until absorbed and scattered by particles accumulated at the chemolimnion (e.g., bacteria, phytoplankton), transformed to heat and trapped within the density interface.

Low turbidity (Fig. 2F) and field observations by the SCUBA divers indicate that light penetrates through the mixolimnion of Nohoch Hol down to 9.0 m water depth and is lost below. In contrast, sites with intense biological activity with turbid mixolimnia, such as Cenote Verde, do not have thermal anomalies. In Verde, the mixolimnion is turbid inhibiting light transmission to the chemolimnion, and in any case there is negligible potential for incident sunlight on the chemolimnion due to the underwater overhanging site morphology (Fig. 7B) (Wilson & Morris, 1994). Thermal anomalies may also be absent, even with transparent mixolimnia, as is the case in Cenote Angelita. While the mixolimnion in Angelita is transparent and the chemolimnion well-positioned to be exposed to penetrating sunlight, the depth of the chemolinion, however, is nearing the light extinction depth ($\sim$20 m) such that only limited heliothermic energy would reach the chemolimnion.

Density

Even with the temperature maximum in the chemolimnion in Nohoch Hol, a very stable density profile is observed (Fig. 2G). For the mixolimnion the calculated densities were 0.999 and 1.024 kg l^{-1} in the monimolinion waters where the salinity gradient is much more significant at determining the density than is the temperature (Fofonoff & Millard, 1983).

Dissolved oxygen

Nohoch Hol has an aerobic mixolimnion conditions with DO ranging from 1.0 to 7.3 mg l^{-1}, a dysoxic (0.1–1 mg l^{-1}) to anoxic chemolimnion with readings below the 0.2 mg l^{-1} detection limit for Hydrolab's DO sensor, and finally, an anoxic monimolimnion. Anaerobic conditions and the occurrence of sulfide and multiple sulfate reduction reactions (Stoessell et al., 1993, 2002; Socki et al., 2002) result in the formation of purplish to red layers, the white haze, and the odor of rotten eggs commonly observed by divers in the Yucatan lentic pit cenotes (e.g., Wilson & Morris, 1994; Stoessell et al., 2002). In the Yucatan Peninsula, sulfate has been shown to be the most important oxidant in modified marine water, with isotopic determinations showing the source to be both the intruding marine waters, as well as dissolution of gypsum minerals (Perry et al., 2009). Evidence of sulfide and sulfate reactions and anoxic conditions have been found outside the Yucatan, such as in Bundera Sinkhole in north-west Australia (Humphreys, 1999; Seymour et al., 2007) and Turks and Caicos Island Bahamas (Koenemann et al., 2004). Similarly, stygobiont cave-dwelling fauna are reported for wide ranging monimolimnia of the Yucatan and elsewhere. These include the fish *Typhliasina pearsei* (Hubbs, 1938) and the shrimp *Creaseria morleyi* (Creaser, 1936) Calica Grande and Cenote Verde (Wilson & Morris, 1994; Skiles et al., 1997), while published reports exist for meromictic systems of the Bahamas and north-west Australia (Table 5; Goehle & Storr, 1977; Humphreys, 1999; Humphreys et al., 1999; Koenemann et al., 2004). These monimolimnia of Yucatan cenotes and anchialine pools elsewhere with dysoxic conditions and sulfide are considered of significant ecological interest due to their separation from the oxygenated atmosphere, adaptations, and the

potential for chemosynthesis (Fenchel & Finlay, 1995).

pH

The slightly basic pH values in the Nohoch Hol surface waters (Fig. 2E) are understood in the context of evaporation and active photosynthesis that consume CO_2, but is relatively lower than in other cenotes where fresh water (i.e., <3 g l^{-1}) at the surface reach $\sim$8 pH units (Socki et al., 2002).

Within the chemolimnion of Nohoch Hol, the pH range is consistent with other meromictic cenotes in the Carribean coast (Wilson & Morris, 1994; Stoessell et al., 1993). Xcolac, an inland meromictic Yucatan cenote (Fig. 1), has two zones with pH variations within the chemolimnion. The uppermost is marked by a pH minimum (6.7) and interpreted as a sulfide oxidation zone (Socki et al., 2002). The second change show a pH maximum (7.1) interpreted as a sulfate reduction region (Dickman & Thode, 1990; Socki et al., 2002).

According to Socki et al. (2002), sulfide or elemental sulfur oxidation take place at 6.7, however, this pH value in Nohoch Hol is found where DO concentration is $\leq$0.2 mg l^{-1}. A possible explanation is that the photosynthetic activity within the chemolimnion consumes CO_2 thus increasing the pH. Deeper within the chemolimnion the decomposition of organic matter reduces the pH. There is an increase in pH towards the base of the monimolimnion most probably related to the marine water characteristic pH (Fig. 2E).

Dissolution of carbonate rocks with different composition (i.e., gypsum) and the precipitation of some elements (i.e., iron) are also important to understand the pH equilibrium in cenotes (Stoessell et al., 1993; Socki et al., 2002). This may be of particular relevance for Nohoch Hol given its location close to the hydrogeochemical transition zone from bicarbonate dominated groundwaters to the north, to groundwaters with sulfate ions from gypsum dissolution (Perry et al., 2002, 2009).

Nutrients

Data on nutrients from meromictic lentic cenotes and even for lotic cenotes are scarce. In Nohoch Hol, the N-NO_3 was the dominant nitrogen species in the mixolimnion while N-NH_4 dominates below it as expected from an oxic–anoxic top-bottom gradient (Fig. 3A; Table 2).

The low concentration of nitrates measured in Nohoch Hol contrast with the high nitrate concentrations of 1100–1300 μM reported for urban and polluted areas near Merida (Herrera-Silveira, 1994; Marín & Perry, 1994; Pacheco & Cabrera, 1997). Nitrate concentrations in Nohoch Hol were lower than in other meromictic pit cenotes of the Yucatan Peninsula including Calica Grande (150 μM) and Angelita (170 μM) (Stoessell et al., 1993), and similar (24 μM) to the meromictic Bundera sinkhole located in north-west Australia (Humphreys, 1999).

Data for ammonia concentration in cenotes are only available for lotic conduit sites and fall within a range of 1.5–8.3 μM N-NH_4 (Alcocer et al., 1999) while Nohoch Hol concentration is higher at 16.7 μM at the chemolimnion and monimolimnion. Such higher ammonium concentrations are expected in lentic waters due to the comparatively longer residence times.

The low SRP is consistent with previous findings on Yucatan Peninsula aquatic systems (Alcocer et al., 1998, 1999) as the carbonate environment favors the co-precipitation of phosphate with calcium (Margalef, 1983). Finally, SRSi was found to be an abundant element, as previously documented in other aquatic systems throughout the Yucatan Peninsula (Alcocer et al., 1998; Herrera-Silveira et al., 1998).

Within the chemolimnion, the alternation of maxima and minima between N-NO_3 and N-NH_4 matches the bacterioplankton bimodal profile suggesting bacterial denitrification at 10 and 12 m depth; however, the N-NO_3 minimum at 10 m may also be related to its consumption by phytoplankton. On the other hand, the N-NO_3 maximum at 11 m suggests oxidation of N-NH_4, a bacterially mediated process called nitrification. The occurrence of nitrification processes has been described for anchialine systems (Pohlman et al., 1997; Humphreys, 1999), but in Nohoch Hol sunlight penetrates to at least 11 m depth as seen in the phytoplankton abundance. Therefore, photosynthesis rather than chemosynthesis seems to be the favored energy production pathway, and N-NH_4 oxidation could be spontaneous due to oxygen released between 10 and 11 m by phytoplankton.

Nohoch Hol could be classified as ultraoligotrophic to oligotrophic according to its low nutrient

concentration (Table 2) when compared with the ranges for tropical lakes (Salas & Martino, 1988). This finding is consistent with the review of 30 cenotes of the Yucatan Peninsula provided by Schmitter-Soto et al. (2002) where the majority was in the oligo-mesotrophic range, and only 15% eutrophic. Even though nitrogen is found in low concentration in Nohoch Hol, the even lower phosphorous concentration explains the role of phosphorous as the limiting nutrient since the N:P Redfield ratio is >16.

Bacterioplankton

The bacterioplankton density in Nohoch Hol is low, with a range of 8.3–35.2 $\times$ 10^3 cell ml^{-1}, which is comparable to the 8 $\times$ 10^3 cells ml^{-1} reported by Alcocer et al. (1999) for anchialine flooded cave systems and the 3.4 $\times$ 10^3 cells ml^{-1} in the associated lotic cenotes (Table 3). Alcocer et al. (1999) identified these bacterioplankton densities as being very low, even for oligotrophic systems. Similarly low densities of 10^2–10^4 cells ml^{-1} have also been reported for other oligotrophic (Ochs et al., 1995) and karstic (Gounot, 1994) water bodies.

The low bacterioplankton densities in oligotrophic cenotes of the eastern Yucatan peninsula are probably related to the scarce phosphorus availability and thus a low autochthonous primary production (Alcocer et al., 1999). However, Schwabe & Herbert (2004) reported higher densities over a range of $\sim$1 to 5 $\times$ 10^7 viable cells ml^{-1} at the meromictic Black Hole in the Bahamas.

The microbial taxonomy of the cenotes and anchialine systems of the Yucatan peninsula is poorly known; nevertheless, some speculations have been previously made regarding the role of the filamentous bacteria like *Beggiatoa* and *Thiothrix* and like the bacillus *Chromatium* on the sulfur cycle, and such as *Thiobacillus* and the family Rhodosperillaceae on the nitrogen cycle (Stoessell et al., 1993, 2002; Wilson & Morris, 1994). Brigmon et al. (1994) identified *Thiothrix*, *Beggiatoa,* and others colorless sulfur bacteria from a Florida aquifer, proposing a model for the sulfur cycle and the microbial ecology for karst aquifers like those from Florida and Yucatan.

The bacterioplankton of the meromictic Devil's Hole, Bahamas, include *Chlorobium*, *Chromatium*, *Thiocystis* and green and purple sulfur bacteria (Goehle & Storr, 1977). The purple sulfur bacteria *Allochromatium* and *Thiocapsa* are the dominant members in the chemolimnion of the meromictic Black Hole, the Bahamas (Schwabe & Herbert, 2004; Herbert et al., 2005), while the sulfur-oxidizing bacteria *Beggiatoa* occurr at the dysoxic marine waters in blue holes (Jorgensen & Revsbech, 1983). Humphreys (1999) and Humphreys et al. (1999) propose that filamentous and rod-shape bacteria like *Beggiatoa, Thiothrix, Sphaerotilus, Thioploca* could be present in the meromictic Bundera sinkhole, Australia, where Seymour et al. (2007) have also documented a complex community of heterotrophic bacteria and viruses.

A bacterial succession is suggested here for Nohoch Hol, controlled by DO concentration and available oxidative power. Within the dysoxic zone at the top of the chemolimnion, colonies of *Beggiatoa* and/or *Thiothrix*, or similar, could actively process sulfur increasing the activity of the sulfur cycle. Deeper within the chemolimnion, *Thiobacillus*-like and other Rhodosperillaceae may be driving the nitrogen cycle. At the anoxic monimolimnion, the rod-shape bacteria similar to *Allochromatium* of the sulfur cycle must be dominant drivers of the nitrogen cycle, while bacteria like *Desulfovibrio*, *Chromatium*, and *Thiocapsa* (coccus) could drive the sulfur cycle.

Phytoplankton

Phytoplankton taxa found in Nohoch Hol are similar to those reported from other cenotes of the Yucatan Peninsula (e.g., López-Adrián & Herrera-Silveira, 1994; Díaz-Arce et al., 2001; Sánchez et al., 2002; Schmitter-Soto et al., 2002); similarly, Chorophyceae was found to be the dominant taxon (Schmitter-Soto et al., 2002). Beyond the Yucatan Peninsula, diatoms had also been reported from the mixolimnion of the Devil's Hole, the Bahamas (Goehle & Storr, 1977). Alternatively, the dominant phytoplankton in the mixolimnion of a similar system in Bundera sinkhole is the chlorophyte *Rhizoclonium* and the charophyte *Lamprothamnium papulosa* (Humphreys, 1999). Charophytes have not been reported yet from the cenotes of the Yucatan Peninsula (López-Adrián & Herrera-Silveira, 1994; Díaz-Arce et al., 2001; Sánchez et al., 2002).

While the total phytoplankton density in Nohoch Hol of 21.9 $\times$ 10^3 cells ml^{-1} has similar density

values of other oligotrophic- and lentic-cenote studied in the northwest Yucatan Peninsula such as Xtogil (19 cells ml^{-1}) and Ixin-Ha (1.6×10^4 cells ml^{-1}), it is suggested that the low diversity in Nohoch Hol is due to the dominance of the single taxon *Scenedesmus* (Díaz-Arce et al., 2001) (Table 4). In comparison, to the 11 taxa in Nohoch Hol, other cenotes of the Yucatan Peninsula have 32 and 88 taxa with up to 150 species (López-Adrián & Herrera-Silveira, 1994; Sánchez et al., 2002; Schmitter-Soto et al., 2002) (Table 4). The low phytoplankton density supports the oligotrophic status suggested by the scarce nutrient concentration.

Similarity and PCA

The isolation of the 10 m depth sample into an independent cluster is a consequence of this depth corresponding to an ecotone characterized with the sharpest environmental gradient (Fig. 2), and the extreme biological aggregation and chemical maxima/minima in the water column (Figs. 3, 4; Table 2). This ecotone, or contact zone, between the surface and bottom habitats has been often characterized by a high biodiversity and biological activity (Vervier et al., 1992) that mediates the transformations of water chemistry through geochemical gradients and microbial biofilms and aggregates (Hancock et al., 2005). The upper boundary of the chemolimnion is shown to be a narrow and extreme environment within the water column.

The clustering of depths 11 m through to 16 m (Fig. 5) underlines persistent depletion of oxygen as a significant factor (Fig. 2C), despite the other differences through this depth range. The vertical trends of light intensity, oxygen saturation, and temperature create biogeochemical gradients (Goldscheider et al., 2006). While the closeness and short linkage distances between Group 1 mixolimnion depths with the Group 2 chemo + monimolimnion is surprising, it points to turbidity and all the factors cross-correlated to turbidity as important given the common low turbidity values (Fig. 2F), in sharp contrast to the extreme turbidity values identified only in Group 3 at the 10 m depth. From our results it is clear that the 10 m depth is an important ecotone that was clearly recognized by the multivariate analysis tests. It is the boundary where matter is retained and undergoes transformation by the microbial biocenoses working as a sink of carbon where higher activities can be measured (Goldscheider et al., 2006). The flux of matter and energy between surface and bottom waters must occur across this vertically restricted ecotone at 10 m (Humphreys, 2006), and is controlled by hydrology and aerobic and anaerobic processes (Vervier et al., 1992). There is decreasing high-value energetic matter in the bottom waters, organic matter is scarce and refractory, and the aquatic domain is generally hypoxic or anoxic. This extreme environment has been metaphorically called the zone of the black-hole sinks (Hancock et al., 2005).

Conclusions

Nohoch Hol is a near-lentic, ectogenetic meromictic cenote. The three typical layers are recognized are: an aerobic mixolimnion, a chemolimnion with sharp physic-chemical gradients, and an arguably anoxic monimolimnion. The electrical conductivity of the mixolimnion indicates some mixing between the lower mixolimnion and the upper chemolimnion waters; the monimolimnion electrical conductivity is similar to that of the Yucatan coastal waters.

The water column structure includes a thermal maximum in the chemolimnion most likely due to heliothermic heating as the sharp density change at the chemolimnion constitute a physical barrier that is efficient at retaining particulate organic matter that along with phyto and bacterioplankton acts as solar radiation trap.

Bacterioplankton and phytoplankton concentrate at the top of the chemolimnion, where light and nutrients are available. Phytoplankton species richness and diversity are low even compared to other Yucatan Peninsula cenotes.

The top of the chemolimnion has the sharpest density gradient within the water column, and acts as a physical barrier to the exchange of dissolved and particulate matter between the mixo and the monimolimnion. This layer is an ecological zone with a crucial role in the biogeochemistry of Nohoch Hol. The multivariate analysis confirmed this role through identifying, for example, contrasting turbidity and dissolved oxygen above and below this layer, as well as the density of bacterioplankton and phytoplankton aggregated at the top of the chemolimnion as the main variables explaining over 85% of the variance.

Based on the low nutrient concentration and low abundance of phytoplankton and bacterioplankton Nohoch Hol could be considered an ultraoligotrophic to oligotrophic water body according to the ranges known for tropical lakes which is consistent to other studies in Yucatan as mentioned before. Phosphorus is the most likely phytoplankton growth limiting nutrient as suggested by the N:P Redfield ratio >16.

Acknowledgments Financial support was provided by the Dirección General de Asuntos del Personal Académico de la Universidad Nacional Autónoma de México through the Project PAPIIT-IN203894 "Ecología y biodiversidad de un sistema anquihalino basado en la producción quimioautotrófica". The authors thank: L. Peralta, M. Sánchez, L.A. Oseguera (PILT, FES Iztacala, UNAM), and V. Urbieta for field and laboratory assistance; B. Phillips and the QRSS for invaluable data and comments on Nohoch Hol underwater exploration and survey; and E. Monroy-Rios for drafting Fig. 1c. The comments from reviewers Eugene Perry and William Humphreys were valuable in significantly improving this communication.

References

Alcocer, J., A. Lugo, E. Marín & E. Escobar, 1998. Hydrogeochemistry of water from five cenotes and evaluation of their suitability for drinking-water supplies, Northeastern Yucatan, México. Hydrogeology Journal 6: 293–301.

Alcocer, J., A. Lugo, M. R. Sánchez, E. Escobar & M. Sánchez, 1999. Bacterioplankton from cenotes and anchialine caves of Quintana Roo, Yucatan Península, México. Revista de Biología Tropical 47: 73–80.

Barbosa, F. A. R. & J. Padisák, 2002. The forgotten lake stratification pattern: atelomixis, and its ecological importance. Verhandlungen Internationale Vereinigung für Theoretische und Angewandte Limnologie 28: 1385–1395.

Beddows, P. A., 1999. Conduit hydrogeology of a tropical coastal carbonate aquifer: Caribbean coast of the Yucatan Peninsula. McMaster University, M.Sc. Thesis.

Beddows, P. A., 2003. Yucatán Phreas, Mexico. In Gunn, J. (ed.), Encyclopaedia of Cave and Karst Science. Routledge Taylor & Francis Group, New York: 794–796.

Beddows, P. A., 2004. Groundwater hydrology of a coastal conduit carbonate aquifer: Caribbean coast of the Yucatán Península, México. University of Bristol, Ph.D. Thesis.

Beddows, P., P. L. Smart, F. F. Whitaker & S. L. Smith, 2002. Density stratified groundwater circulation on the Caribbean coast of the Yucatán peninsula, México. Karst Waters Institute Special Publication 7: 129–134.

Beddows, P. A., P. L. Smart, F. F. Whitaker & S. L. Smith, 2007. Decoupled fresh–saline groundwater circulation of a coastal carbonate aquifer: spatial patterns of temperature and specific electrical conductivity. Journal of Hydrology 346: 18–32.

Borcard, D., F. Gillet & P. Legendre, 2011. Numerical Ecology. Springer Science, New York.

Boulton, A. J., G. D. Fenwick, P. J. Hancock & M. S. Harvey, 2008. Biodiversity, functional roles and ecosystem services of groundwater invertebrates. Invertebrate Systematics 22: 103–116.

Brigmon, R. L., H. M. Martin, T. L. Morris, G. Bitton & S. G. Zam, 1994. Biogeochemical ecology of *Thiothrix* spp. in underwater limestone caves. Geomicobiology Journal 12: 141–159.

Butterlin, J. & F. Bonet, 1963. Las formaciones cenozoicas de la parte mexicana de la peninsula de Yucatán. Ingenieria Hidráulica en México 17: 63–71.

Cole, G. A., 1979. Textbook of Limnology. The CV Mosby Company, St. Louis.

Connors, M., A. R. Hildebrand, M. Pilkington, C. Ortiz Aleman, R. E. Chavez, J. Urrutia Fucugauchi, E. GranielCastro, A. Camara Zi, J. Vasquez & J. F. Halpenny, 1996. Yucatan karst features and the size of Chicxulub crater. Geophysical Journal International 127: F11–F14.

Díaz-Arce, V., J. A. Herrera-Silveira & F. A. Comín, 2001. Limnological characteristics of two types of cenotes of Yucatan. Verhandlungen Internationale Vereinigung für Theoretische und Angewandte Limnologie 27: 3579–3582.

Dickman, M. D. & H. G. Thode, 1990. Sulfur bacteria and sulfur isotope fractionation in a meromictic lake near Toronto, Canada. In Ihebhot, V., S. Kempe, W. Michaelis & A. Spitzg (eds), Facets of Modem Biochemistry. Springer-Verlag, Berlin: 225–241.

Doehring, D. O. & J. H. Butler, 1974. Hydrogeologic constraints on Yucatan′s development. Science 186: 591–595.

Fenchel, T. & B. J. Finlay, 1995. Ecology and Evolution in Anoxic Worlds. Oxford University Press, New York.

Fetter, C. W. Jr., 1972. Position of the saline water interface beneath oceanic islands. Water Resources Research 8: 1307–1314.

Fetter, C. W., 1994. Applied Hydrogeology, 3rd ed. Prentice Hall, New Jersey.

Flores, S. & I. Espejel, 1994. Tipos de vegetación de la Península de Yucatán. Entomoflora Yucatanense. Vol. 3. Universidad Autónoma de Yucatán, México.

Fofonoff, N. P., 1985. Physical properties of seawater: a new salinity scale and equation of state of seawater. Journal of Geophysical Research 90: 3332–3342.

Fofonoff, N. P. & R. C. Millard Jr., 1983. Algorithms for computation of fundamental properties of seawater, UNESCO technical paper in marine science 44, UNESCO.

García, E., 1973. Modificación al sistema de clasificación climática de Köeppen. Para adaptarlo a las condiciones de la República Mexicana. Instituto de Geografia UNAM, Mexico.

Garman, M. & J. Garey, 2005. The mysterious clouds of Jewfish Sink. National Association for Cave Diving Journal 38: 7–8.

Gauch, H. G., 1982. Multivariate Analysis in Community Ecology. Cambridge University Press, Cambridge.

Glover, L. K. & S. A. Earle, 2004. Defying Ocean's End: An Agenda for Action. IUCN-Island Press, Washington, DC.

Goehle, K. H. & J. F. Storr, 1977. Biological layering resulting from extreme meromictic stability, Devil's Hole, Abaco Island, Bahamas. Internationale Vereinigung fur Theoretische und Angewandte Limnologie 20: 550–555.

Goldscheider, N., D. Hunkeler & P. Rossi, 2006. Microbial biocenoses in pristine aquifers and an assessment of investigative methods. Hydrogeology Journal 10: 1–16.

Gounot, A. M., 1994. Microbial ecology of groundwaters. In Gibert, J., D. L. Danielopol & J. A. Stanford (eds), Groundwater Ecology. Academic Press, London: 189–215.

Hancock, P. J., A. J. Boulton & F. William, 2005. Humphreys aquifers and hyporheic zones: towards an ecological understanding of groundwater. Hydrogeology Journal 13: 98–111.

Herbert, R., A. Ranchou-Peyruse, R. Duran, R. Guyoneaud & S. Schwabe, 2005. Characterization of purple sulfur bacteria from the South Andros Black Hole cave system: highlights taxonomic problems for ecological studies among the genera *Allochromatium* and *Thiocapsa*. Environmental Microbiology 7: 1260–1268.

Herrera-Silveira, J. A., 1994. Nutrients from underground water discharges in a coastal lagoon (Celestun, Yucatan, Mexico). Verhandlungen Internationale Vereinigung für Theoretische und Angewandte Limnologie 25: 1398–1401.

Herrera-Silveira, J. A., F. A. Comín, S. López & I. Sánchez, 1998. Limnological characteristics of aquatic ecosystems in Yucatan Peninsula (SE Mexico). Verhandlungen Internationale Vereinigung für Theoretische und Angewandte Limnologie 26: 1348–1351.

Hildebrand, A. R., M. Pilkington, M. Connors, C. Ortiz Aleman & R. E. Chavez, 1995. Size and structure of the Chicxulub Crater revealed by horizontal gravity gradients and cenotes. Nature 376: 415–417.

Humphreys, W. F., 1999. Physico-chemical profile and energy fixation in Bundera Sinkhole, an anchialine remiped habitat in north-western Australia. Journal of the Royal Society of Western Australia 82: 89–98.

Humphreys, W. F., 2006. Aquifers: the ultimate groundwater-dependent ecosystems. Australian Journal of Botany 54: 115–132.

Humphreys, W. F., A. Poole, S. M. Eberhard & D. Warren, 1999. Effects of research diving on the physico-chemical profile of Bundera Sinkhole, an anchialine remiped habitat at Cape Range, Western Australia. Journal of the Royal Society of Western Australia 82: 99–108.

Hutchinson, G. E., 1957. A Treatise on Limnology Volume 1. Wiley, New York.

Iliffe, T. M., 2000. Anchialine cave ecology. In Wilkens, H., D. C. Culver & W. F. Humphreys (eds), Ecosystems of the World. 30. Subterranean Ecosystems. Elsevier Science, Amsterdam: 57–75.

Instituto de Geografia, Universidad Nacional Autónoma de México, 1973. Climas: Precipitación y probabilidad de la lluvia en la Republica Mexicana y su evaluación: Precipitación y probabilidad de lluvia en los Estados de Campeche, Yucatán y Quintana Roo. CETENAL—Comision de Estudios del Territorio Nacional, México DF.

Jorgensen, B. B. & N. Revsbech, 1983. Colourless sulfur bacteria, *Beggiatoa* spp. in O_2 and H_2S microgradients. Applied and Environmental Microbiology 45: 1261–1270.

Koenemann, S., T. M. Iliffe & J. Yager, 2004. *Kaloketos pilosus*, a new genus and species of Remipedia (Crustacea) from the Turks and Caicos Island. Zootaxa 618: 1–12.

Lampert, W. & U. Sommer, 1997. Limnoecology: The Ecology of Lakes and Streams. Oxford University Press, NY.

Legendre, P. & L. Legendre, 1998. Numerical Ecology. Elsevier, Amsterdam.

Lewis, W. M., 1973. The thermal regime of lake Lanao (Philippines) and its theoretical implications for tropical lakes. Limnology and Oceanography 18: 200–217.

Lewis, W. M. Jr., 1983. A revised classification of lakes based on mixing. Canadian Journal of Fisheries and Aquatic Sciences 40: 1779–1787.

Lewis, W. M. Jr., 1996. Tropical lakes: how latitude makes a difference. In Shiemer, F. & K. T. Boland (eds), Perspectives in Tropical Limnology. Academic Publishing, Amsterdam: 43–64.

López-Adrián, S. & J. A. Herrera-Silveira, 1994. Plankton composition in a cenote, Yucatán México. Verhandlungen Internationale Vereinigung für Theoretische und Angewandte Limnologie 25: 1402–1405.

Lopez-Ramos, E., 1975. Geological summary of the Yucatán Peninsula. In Nairn, A. E. M. & F. G. Stehli (eds), The Ocean Basin and Margin. III. The Gulf of Mexico and the Caribbean. Plenum, New York: 257–282.

Margalef, R., 1983. Limnología. Omega, Barcelona.

Marín, L. E. & E. C. Perry, 1994. The hydrogeology and contamination potential of northwestern Yucatán, México. Geofisica Internacional 33: 619–623.

Merino Ibarra, M. & L. Otero Dávalos, 1991. Atlas Ambiental Costera: Puerto Morelos, Quintana Roo. Instituto de Ciencias del Mar y Limnologia, UNAM, Centro de Investigaciones de Quintana Roo, Mexico, DF.

Metcalfe, C. D., P. A. Beddows, G. G. Gold, T. L. Metcalfe, H. Li & H. van Lavieren, 2011. Contaminants in the coastal karst aquifer system along the Caribbean coast of the Yucatan Peninsula, Mexico. Environmental Pollution 159: 991–997.

Moore, Y. H., R. K. Stoessell & D. H. Easley, 1992. Freshwater/sea-water relationship within a ground-water flow system, Northeastern Coast of the Yucatan Peninsula. Ground Water 30: 343–350.

Moore, Y. H., R. K. Stoessell & D. H. Easley, 1993. Reply to discussion of "Fresh-water/sea-water relationship within a ground-water flow system, Northeastern Coast of the Yucatan Peninsula". Ground Water 31: 321–322.

Ochs, C. A., J. J. Cole & G. E. Likens, 1995. Population dynamics of bacterioplankton in an oligotrophic lake. Journal of Plankton Research 17: 365–391.

Pacheco, J. A. & S. A. Cabrera, 1997. Groundwater contamination by nitrates in the Yucatán Peninsula, México. Hydrogeology Journal 5: 47–53.

Parsons, T. R., Y. Maita & C. M. Lalli, 1984. A Manual of Chemical and Biological Methods of Seawater Analysis. Pergamon Press, London.

Perry, E., L. Marín, J. McClain & G. Velázquez, 1995. Ring of cenotes (sinkholes), northwest Yucatan, Mexico: Its hydrogeologic characteristics and possible association with the Chicxulub impact crater. Geology 23: 17–20.

Perry, E., G. Velazquez-Oliman & L. Marin, 2002. The hydrogeochemistry of the karst aquifer system of the Northern Yucatan Peninsula, Mexico. International Geology Review 44: 191–221.

Perry, E., A. Paytan, B. Pedersena & G. Velazquez-Oliman, 2009. Groundwater geochemistry of the Yucatan Peninsula, Mexico: constraints on stratigraphy and hydrogeology. Journal of Hydrology 367: 27–40.

Pindell, J. L., 1994. Evolution of the Gulf of Mexico and the Caribbean. In Donovan, S. K. & T. A. Jackson (eds), Caribbean Geology: An Introduction. University of the West Indies Publisher's Association, Kingston: 13–39.

Pohlman, J. W., T. M. Iliffe & L. A. Cifuentes, 1997. A stable isotope study of organic cycling and the ecology of an anchialine cave ecosystem. Marine Ecology Progress Series 155: 17–27.

Pope, K. O., S. C. Ocampo, G. L. Kinsland & R. Smith, 1996. Surface expression of the Chicxulub crater. Geology 24: 527–530.

Porter, K. G. & Y. S. Feig, 1980. The use of DAPI for identifying and counting aquatic microflora. Limnology and Oceanography 25: 943–948.

QRSS—Quintana Roo Speleological Survey, 2010. Online data base www.caves.org/project/qrss/qrss.htm.

Rzendowski, J., 1981. Vegetación de México. Limusa, México.

Salas, H. J. & P. Martino, 1988. Desarrollo de metodologías simplificadas para la evaluación de eutroficación en lagos cálidos tropicales. Cuarto Encuentro "Eutroficación de lagos tropicales". CEPIS, San Juan de Puerto Rico.

Salas, H. J. & P. Martino, 1991. A simplified phosphorus trophic state model for warm-water tropical lakes. Water Research 25: 341–350.

Sánchez, M., J. Alcocer, E. Escobar & A. Lugo, 2002. Phytoplankton of cenotes and anchialine caves along a distance gradient from northeastern coast of Quintana Roo, Yucatan Península. Hydrobiologia 467: 79–89.

Schmitter-Soto, J. J., F. A. Comin, E. Escobar-Briones, J. Herrera-Silveira, J. Alcocer, E. Suárez-Morales, M. Elias-Gutiérrez, V. Díaz-Arce, L. E. Marin & B. Steinich, 2002. Hydrogeochemical and biological characteristics of cenotes in the Yucatan Península (SE México). Hydrobiologia 467: 215–228.

Schwabe, S. & R. A. Herbert, 2004. Black holes of the Bahamas: what they are and why they are black. Quaternary International 121: 3–11.

SEDUMA (Secretaria de Desarrollo Urbano y Medio Ambiente), 2010. Online data base. www.seduma.yucatan.gob.mx/cenotes-grutas/censo-cenotes.php.

Seymour, J. R., W. F. Humphreys & J. G. Mitchell, 2007. Stratification of the microbial community inhabiting an anchialine sinkhole. Aquatic Microbial Ecology 50: 11–24.

Skiles, W., L. Butt, T. Morris & A. W. Hayes, 1997. A survey of two cenotes and their associated spelean features, within CALICA property, Quintana Roo, México. Karst Environmental Services, Inc., High Springs, Florida.

Smart, P. L., P. A. Beddows, J. Coke, S. Doerr, S. L. Smith & F. F. Whitaker, 2006. Cave development on the Caribbean coast of the Yucatan Peninsula, Quintana Roo, Mexico. Geological Society of America Special Paper 404, Perspectives on Karst Geomorphology, Hydrology, & Geochemistry: 105–128.

Socki, R. A., E. Perry & C. Romanek, 2002. Stable isotope systematics of two cenotes from the northern Yucatan Peninsula, Mexico. Limnology and Oceanography 47: 1808–1818.

Soteres, A. D., 2000. Groundwater model of fresh/salt-water lens in the northeastern Yucatan Peninsula. University of New Orleans, Louisiana, M.Sc. Thesis.

Stirling, H. P., 1985. Chemical and Biological Methods of Water Analysis for Aquaculturists. Institute of Aquaculture, University of Stirling, Scotland.

Stock, J. H., T. M. Iliffe & D. Williams, 1986. The concept "anchialine" reconsidered. Stygologia 2: 90–92.

Stoessell, R. K., W. C. Ward, B. H. Ford & J. D. Schuffert, 1989. Water chemistry and $CaCO_3$ dissolution in the saline part of an open-flow mixing zone, coastal Yucatan Peninsula, Mexico. Bulletin of the Geological Society of America 10: 159–169.

Stoessell, R. K., Y. H. Moore & J. G. Coke, 1993. The occurrence and effect of sulfide oxidation on coastal limestone dissolution in Yucatan Cenotes. Ground Water 31: 566–575.

Stoessell, R. K., J. G. Coke & D. H. Easley, 2002. Localized thermal anomalies in haloclines of coastal Yucatan sinkholes. Ground Water 40: 416–424.

Strickland, J. D. H. & T. R. Parsons, 1972. A practical handbook of seawater analysis. Bulletin Fisheries Research Board Canada 167: 1–310.

Talling, J. F. & J. Lemoalle, 1998. Ecological Dynamics of Tropical Inland Waters. Cambridge University Press, Cambridge.

Tavera, R. & V. Martínez-Almeida, 2005. Atelomixis as a possible driving force in the phytoplankton composition of Zirahuen, a warm-monomictic tropical lake. Hydrobiologia 533: 199–208.

Utermöhl, H., 1958. Zur Vervollkommnung der quantitativen phytoplankton-methodik. Mitteilungen der Internationale Vereinigung für Theoretische und Angewandte Limnologie 9: 1–39.

Vervier, P., J. Gibert, P. Marmonier & M. J. Dole-Olivier, 1992. A perspective on the permeability of the surface freshwater–groundwater ecotone. Journal of the North American Benthological Society 11: 93–102.

Weidie, A. E., 1985. Geology of the Yucatan platform. In: Ward W. C., A. E. Weidie & W. Ward (eds), Geology and Hydrogeology of the Yucatan and Quaternary Geology of Northeastern Yucatan Peninsula. Orleans Geological Society, New Orleans: 1–12.

Wetzel, R. G., 2001. Limnology. Academic Press, New York.

Wetzel, R. G. & G. E. Likens, 1979. Limnological Analyses. Saunders, Philadelphia.

Whitaker, F. F. & P. L. Smart, 1997. Groundwater circulation and geochemistry of a karstified bank-marginal fracture system, South Andros Island. Bahamas Journal of Hydrology 197: 293–314.

Wilson, E. M., 1980. Physical geography of the Yucatán Peninsula. In Moseley, E. & E. Terry (eds), Yucatán. A World Apart. University of Alabama Press, Tuscaloosa: 5–40.

Wilson, W. L. & T. L. Morris, 1994. Cenote Verde: a Meromictic karst pond, Quintana Roo, México. In Sasowsky, I. D. & M. V. Palmer (eds), Breakthroughs in Karst Geomicrobiology and Redox Geochemistry. Karst Waters Institute Special Publication 1, Colorado: 77–79.